Published in final edited form as:
AJNR Am J Neuroradiol. 2018 April ; 39(4): 713–719. doi:10.3174/ajnr.A5546.

Quantification of intracranial aneurysm volume pulsation with 7T MRI

Rachel Kleinloog, MD[1], **Jaco J Zwanenburg, PhD**[2], **Bram Schermers, BS**[1,3], **Erwin Krikken, BS**[1,3], **Ynte M Ruigrok, MD, PhD**[1], **Peter R Luijten, PhD**[2], **Fredy Visser**[2,4], **Luca Regli, MD, PhD**[1,5], **Gabriel JE Rinkel, MD**[1], and **Bon H Verweij, MD, PhD**[1]

[1]Brain Center Rudolf Magnus, Department of Neurology and Neurosurgery, Utrecht University, University Medical Center Utrecht, Utrecht, The Netherlands [2]Department of Radiology, Utrecht University, University Medical Center Utrecht, Utrecht, The Netherlands [3]Faculty of Science and Technology, Department of Technical Medicine, University of Twente, Enschede, The Netherlands [4]Philips Healthcare, Best, The Netherlands [5]Department of Neurosurgery, University Hospital Zurich, Zurich, Switzerland

Abstract

Background and purpose—Aneurysm volume pulsation is a potential predictor of intracranial aneurysm rupture. We evaluated whether 7T MRI can quantify aneurysm volume pulsation.

Materials and Methods—In stage I of the study, ten unruptured aneurysms in nine patients were studied using a high resolution (0.6 mm, isotropic) 3D gradient-echo sequence with cardiac gating. Semi-automatic segmentation was used to measure aneurysm volume (in mm^3) per cardiac phase. Aneurysm pulsation was defined as the relative increase in volume between the phase with the smallest volume and the phase with the largest volume. The accuracy and precision of the measured volume pulsations was addressed by digital phantom simulations, and a repeated image analysis. In stage II, the imaging protocol was optimized and nine patients with nine aneurysms were studied with and without administration of a contrast agent.

Results—The mean aneurysm pulsation in stage I was 8% (standard deviation (SD) 7%, range 2 to 27%), with a mean volume change of 15 mm^3 (SD 14 mm^3, range 3 to 51 mm^3). The mean difference in volume change for the repeated image analysis was 2 mm^3 (SD 6 mm^3). The artifactual volume pulsations measured with the digital phantom simulations were in the same magnitude as the volume pulsations observed in the patient data, even after protocol optimization in stage II.

Conclusion—Volume pulsation quantification with the current imaging protocol on 7T MRI is not accurate due to multiple imaging artifacts. Future studies should always include aneurysm-specific accuracy analysis.

Corresponding author: Rachel Kleinloog, Brain Center Rudolf Magnus, Department of Neurology and Neurosurgery, room G. 03.232. Utrecht University, University Medical Center Utrecht, Utrecht, The Netherlands Heidelberglaan 100, 3584 CX Utrecht, The Netherlands, Tel: +3188-7555555 | Fax: +3130-2542100 | rachelkleinloog@gmail.com.

Europe PMC Funders Author Manuscripts

Europe PMC Funders Author Manuscripts

Introduction

Intracranial aneurysms occur in approximately 3% of the population.1 Rupture of an aneurysm results in aneurysmal subarachnoid hemorrhage (SAH), which often occurs at a younger age and has a high case fatality and morbidity.2 Current standard treatment consists of neurosurgical clipping or endovascular coiling, and can prevent rupture, but carries a 4 to 8% risk of major complications including death, depending on age of the patient, and size and site of the aneurysm.3,4 Preventive treatment should therefore ideally be restricted to those patients that have a high risk of rupture. However, prediction of the risk of rupture of intracranial aneurysms is poor. Therefore, better predictors of rupture are needed. Volume pulsation, the change in volume during the cardiac cycle, is a potential predictor of rupture.5 Imaging techniques used thus far in attempts to visualize volume pulsation, such as 1.5T phase –contrast MR angiography, transcranial Doppler ultrasound, 3D rotational angiography, and 4D CTA, have various limitations, including limited signal-to-noise ratio (SNR), limited spatial resolution compared to the aneurysm volume, and/or the use of a radiation dose and/or the risk of complications.5 Furthermore, a test of the accuracy and the precision of the volume pulsation measurement was either lacking or studies refrained from giving an error value that can be used to interpret the pulsation results for each aneurysm. Therefore, aneurysm volume pulsation is currently not used as a predictor of rupture in clinical practice. In this experimental study, we evaluated whether volume pulsation could be quantified on images obtained with 7T MRI, and tested accuracy and precision of the method.

Materials and Methods

Our study consisted of two stages. In the first stage, we tested the concept of quantification of aneurysm pulsation on images obtained with 7T MRI, and we tested the accuracy and repeatability of the imaging analysis method. In the second stage, we implemented the lessons learned in stage I to optimize the imaging protocol and accuracy of the quantification of aneurysm pulsation.

Study population

Patients diagnosed with saccular intradural unruptured intracranial aneurysms who were either planned for treatment of their aneurysm or were in follow-up for growth of their aneurysm, were recruited through our outpatient clinic of the department of Neurology and Neurosurgery between July 2011 and December 2012 as part of an existing study focusing on imaging of the aneurysm wall (stage I).6 In stage II, additional patients were recruited for the purpose of the current study between February and April 2014. The diagnosis of the aneurysm was made either on CTA or 1.5 or 3.0 Tesla MRA, and the aneurysms were either incidental findings (imaging study was made for other indications), found during screening because of a positive family history of intracranial aneurysm, or symptomatic aneurysms (e.g. leading to a seizure or thrombo-embolic event). Patients with contraindications for 7T MRI (e.g. claustrophobia, metal objects such as dental implants or prostheses in or on the body) were excluded, as well as patients with aneurysms associated with vascular malformations other than aneurysms, e.g. arteriovenous malformations. In the second stage,

Europe PMC Funders Author Manuscripts

also patients with renal insufficiency and allergy to gadolinium-based contrast agent were excluded. This study was approved by the Institutional Review Board of our center and all participants gave written informed consent following guidelines equivalent to the National Institutes of Health guidelines.

7T MR Imaging

Imaging was performed on a 7T MRI scanner (Philips Healthcare, Cleveland, OH, USA) with a volume transmit coil and a 32 channel receive head-coil (Nova Medical, Wilmington, MA, USA). In the first stage, the volume pulsation of the aneurysm was studied by adding a 3D Turbo Field Echo sequence (further referred to as TFE) to an existing study focusing on imaging the aneurysm wall.6 This protocol included a low resolution T1 weighted survey sequence and a TOF sequence covering the intracranial vessels from the level of the circle of Willis and upward, taking into account the location of the aneurysm.6 It also included a previously described time-resolved 3D PCMR sequence.7 The following parameters were used in the 3D TFE sequence: TR/TE 8.2/4.4 ms, flip angle 6°, FOV 180 mm x 180 mm x 9.6 mm, an acquired spatial resolution of 0.6 mm x 0.6 mm x 0.6 mm, sensitivity encoding acceleration factor of 2.0 (RL), and an acquired temporal resolution of 90 ms, interpolated to 15 cardiac phases. The sequence was synchronized to the heart with a peripheral pulse unit and retrospective cardiac gating. The scan duration was approximately 4 minutes. The TFE sequence was oriented in either coronal or transverse orientation, depending on the location of the aneurysm in the circle of Willis and its orientation, and carefully positioned over the aneurysm as observed on a TOF and/or low resolution T1 weighted survey. In both the TOF and the TFE sequence, flow compensated gradients were used to prevent signal drop out from fast flowing blood.

With the results of stage I, the imaging protocol was optimized. An optimized version of the TFE sequence was developed and used in the additionally recruited patients in stage II. We increased the FOV, thereby increasing signal to noise ratio and improving coverage; we shortened the TE to 2.0 ms, to decrease the influence of the flow displacement artifact; and we used a 20° flip angle to increase the contrast-to-noise-ratio (CNR) between flowing blood and static tissue. Furthermore, we performed this improved TFE sequence also after administration of Gadobutrol, a gadolinium-based contrast agent, to further increase CNR and decrease the influence of intensity fluctuations due to inflow effects.

Image analysis

Volume pulsation quantification—Image analysis was performed with the use of ANALYZE 11.0 (AnalyzeDirect, Inc., Overland Park, KS, USA), software designed to automatically segment and calculate volumes. For the cardiac phases of each slice (15 phases in the first stage of the study, 18 in the second stage), the same region of interest containing the aneurysm was chosen on the TFE images, using the TOF or T1 weighted survey images as three-dimensional reference to correctly separate the aneurysm from the parent artery. Vessel segmentation (including the aneurysm) was performed by setting a signal intensity threshold. The threshold was defined by R.K. by visual inspection of the aneurysm and its surroundings and after comparing the TFE images with the anatomy of the aneurysm on the TOF and/or low resolution T1 weighted survey. The threshold was adjusted

until the aneurysm was distinguishable from the background, and at the same time had the same appearance as on the anatomical scan. The threshold was set for each aneurysm separately, but fixed for all slices and cardiac phases of each aneurysm. Thereafter the remaining parent vessel was manually deselected (by R.K.) on each slice of the first phase of the cardiac cycle and then this deselected area was copied to the 14 (or 17 in stage II) consecutive phases of the cardiac cycle and removed. Flow artifacts in the lumen of the aneurysm were misrecognized by the software and consequently manually included in the selection, keeping the borders of the aneurysm as selected by the software intact. Voxels selected outside the aneurysm borders due to background noise were also removed from the selection. The manual corrections were done slice by slice. If the signal in the last slice containing the aneurysm was of low intensity due to partial volume effects, it was sometimes difficult to distinguish noise pixels from aneurysm voxels. Consequently, such a slice was excluded in all phases, to limit the effect of noise on the selection. For each phase of the cardiac cycle, the total volume of the aneurysm was calculated by adding up the aneurysm volumes of all slices (segmented area x slice thickness). Absolute volume pulsation was defined as the change in volume (in mm^3) between the phase of the cardiac cycle with the smallest volume and the phase with the largest volume. Relative volume pulsation was calculated with the following formula: ((maximum volume - minimum volume) / minimum volume) * 100.

The size (largest diameter) of the aneurysms was measured on the TOF angiography in the first stage. In the second stage, it was measured on the improved TFE. Partially thrombosed aneurysms were excluded for the image analysis.

Repeatability of the volume pulsation quantification (stage I)—By repeating the volume measurements for the phase with the smallest and the largest volume for each aneurysm, we determined the precision of the pulsation analysis. The repeated analysis was performed by the same observer, but blinded for the initial analysis with a three month interval between the two analyses. We evaluated the repeatability of the image analysis using the Bland-Altman method: the mean and the standard deviation (SD) of the difference between the results of the initial analysis and the results of the repeated analysis were calculated.8 A t-distribution with a significance level of 0.05 and 9 degrees of freedom (10 measured aneurysms) was used to approximate the distribution of the 95% CI. Also, the Pearson correlation coefficient between the initial analysis and the repeated analysis was calculated. The repeatability analysis was only performed in stage I of this study.

Accuracy of the volume pulsation quantification (stage I)—The accuracy of the volume pulsation analysis is expected to depend on four different factors: the CNR (between blood and surroundings) of the images, signal intensity fluctuations in the gated TFE sequence due to inflow effects, aneurysm size, and blood flow artifacts.

CNR, signal intensity fluctuations and aneurysm size

To estimate the influence of CNR, signal intensity fluctuations and aneurysm size on the calculated volume pulsations, digital phantom simulations were performed in which the

three factors that are thought to influence the accuracy were varied. See supplementary material for further details. In these simulations, the CNR was defined as

$$\mathrm{CNR} = \frac{\text{contrast}}{\text{notes}} = \frac{\mu_s - \mu_{bg}}{\sigma_s} \quad \text{[Eq.1]}$$

with μ_s as the mean pixel value in the phantom region, μ_{bg} as the mean pixel value in a background region, both averaged over the time phases in the cardiac cycle (15 in the first stage of the study and 18 in the second stage). σ_s is the mean of the time phase standard deviation of each pixel in the signal phantom region. In the first digital phantom experiment, the dependence of the inaccuracy of the volume pulsation analysis of both CNR and signal fluctuations was studied. Second, the interaction of aneurysm volume with CNR and signal fluctuations was studied by static digital phantom simulations. Third, aneurysm-specific inaccuracy in the pulsation analysis was measured for each aneurysm in the patient study by making pulsating digital phantoms with the same volume, CNR, intensity fluctuation and volume pulsation. The difference in the volume pulsation measured in the digital phantoms, and the volume pulsation that was measured in the patient scans (and was used as input for the phantoms volume pulsation) was called the absolute observed artifactual pulsation.

Flow displacement artifact

In image acquisition, the timing difference between the moment of phase encoding (right after excitation) and the moment of frequency encoding (approximately at t=TE), will lead to the flow displacement artifact.9 We assessed the potential influence of this artifact by combining the TFE images from stage I with images containing blood flow velocity data (obtained with the time-resolved 3D PCMR sequence, only available in stage I, see supplementary material for further details).

Imaging protocol optimization (stage II)—Volume pulsation quantification on images obtained with the improved TFE were analyzed with the same analysis tool used in stage I. As in stage I, the accuracy of the volume pulsation analysis method was addressed in pulsating phantoms. For both the improved TFE and the gadolinium enhanced improved TFE patient data, pulsating phantoms were made to estimate the (aneurysm-specific) inaccuracy in the pulsation. The volume pulsation measurement in the phantom was compared with the given volume pulsation. This difference yielded the absolute observed artifactual pulsation.

Results

An overview of the results of Stage I and II are given in Table 1

Stage I. Volume pulsation quantification, repeatability and accuracy of the analysis—In stage I, the mean aneurysm volume change was 15 mm^3 (SD 14 mm^3, range 3 to 51 mm^3), and the mean volume pulsation was 8% (SD 7%, range 2 to 27%). The mean time between the minimum and the maximum volume was 7 phases (range 2-12). The timing of the minimum and maximum volume within the cardiac cycle was inconsistent

between different patients, with minimum volume followed by maximum volume in some patients, while the maximum was followed by the minimum volume in others (Table 2). Figure 1 shows the 15 images obtained during the cardiac cycle of one cross section of an aneurysm, and a video of this pulsating aneurysm is provided as Supplementary video. The repeatability analysis yielded a correlation coefficient of 0.95 (Figure 2). The mean of the difference between the results of the initial pulsation analysis and the results of the repeated pulsation analysis was 2 mm^3 (SD 6 mm^3, 95% CI -12 to 15, Figure 2).

The absolute observed pulsation in a static digital phantom (used as measure for the inaccuracy of the analysis) was found to increase quickly below a CNR of approximately 6, and increased with increasing signal intensity fluctuations (see supplementary material for further details and figures). The mean CNR of aneurysms in the patient study was 5 (range 1 to 8) while the mean intensity fluctuation was 3% (SD 1.6%). Both the effects of CNR and intensity fluctuations were size dependent, with increasing relative inaccuracy with decreasing phantom volumes. The mean absolute observed artifactual pulsation in the pulsating digital phantoms (used as measure for the inaccuracy of the analysis) was 2.0 mm^3 (SD 1.6 mm^3, range 0.2 to 5.4 mm^3, Table 2, Supplementary table 1). The potential pulsation observed as a result of the flow displacement artifact depended considerably on the orientation of the acquisition. The worst case artefactual pulsation was equal or higher than the actual pulsation measured in four of the six available patient data sets (see Supplementary table 2). The minimum artifactual volume pulsation was around 25% of the volume pulsation measured in the patient scans.

Stage II. Results after imaging protocol optimization—The mean aneurysm volume change on the improved TFE was 38 mm^3 (SD 31 mm^3, range 2 to 88 mm^3), and the mean volume pulsation was 39% (SD 24%, range 14 to 73%). The mean aneurysm volume change on the contrast enhanced improved TFE was 14 mm^3 (SD 9 mm^3, range 1 to 25 mm^3), and the mean volume pulsation was 15% (SD 11%, range 4 to 36%). The mean time between the minimum and the maximum volume was 8 phases (range 3-14) in the improved TFE and 7 (range 3-13) in the contrast enhanced TFE. As in stage I, the timing of the minimum and maximum volume within the cardiac cycle differed between patients (Table 3). The mean CNR was 23 (SD 7) in the improved TFE and 28 (SD 8) in the gadolinium enhanced improved TFE, while the mean intensity fluctuation was 23% (SD 7%) in the improved TFE and 15% (SD 6%) in the gadolinium enhanced improved TFE. The mean absolute observed artifactual pulsation in the pulsating digital phantoms (used as measure for the inaccuracy of the analysis) was 13 mm^3 (SD 9 mm^3, range 1 to 27 mm^3, Table 3 and Supplementary table 3).

Discussion

This study shows that quantification of volume pulsation of unruptured intracranial aneurysms is currently not feasible when using a semi-automatic segmentation method, even on high resolution 7T MR images. The accuracy of the quantification of volume pulsation is influenced by the CNR, intensity fluctuations, aneurysm size and most importantly by the flow displacement artifact. Our study shows that the artifactual volume pulsation due to

these influences is of the same magnitude as the volume pulsations observed in the patient data, even after optimization of the imaging sequences and adding contrast agent.

Three previous studies quantified pulsation in unruptured aneurysms by the use of a ECG-gated CTA.10–12 Two of these studies found a volume pulsation in the range of 3 to 18% with a mean of 8% (SD 5%),10 and in the range of 1 to 15% with a mean of 5% (SD 4%),11 which compares well with our findings. The third study did not report volume pulsations, but focused on feasibility of imaging pulsation by comparing the aneurysm volume curves and random curves with the arterial pulse wave (as a measure for 'true' pulsation) and found that the aneurysm volume curves showed higher similarity with the pulse wave than the random curves, but only in a subset of the aneurysms under study.12 Accuracy and precision analyses were performed in all CTA studies. The first study found a mean of 8% volume pulsation in aneurysms, which was considered substantial in comparison with a 2% volume change found in bone tissue.10 In the second study, a large and static phantom (a syringe filled with saline) was imaged to study the artificial volume pulsation, and it was concluded that its volume change of < 0.248% was an insignificant artifact.11 However, in the current study, we showed that inaccuracy increases with decreasing phantom size, and therefore their accuracy analysis might underestimate the artifactual pulsation, because the phantom used was much larger than the aneurysms studied. The second study measured an interobserver discrepancy in the repeated measurement of 5 aneurysms of 11.9 mm^3 (SD 17.6 mm^3) which was considered acceptable, given a mean expansion volume of all aneurysms of 27.87 mm^3 (SD 60.53 mm^3).11 The third study found an intra- and interobserver variability of around 0.5 of the post-processing method used, which is fair. The first and second study refrained from giving an error value that can be used to interpret the pulsation results for each aneurysm. Our study shows that the error is influenced by multiple artifacts and is aneurysm specific, which makes it difficult to compare the accuracy of 7T MRI with the reported CTA accuracies. Furthermore, CTA has its own technique-specific artifacts which should be taken into account when analyzing accuracy of the pulsation measurement.5

We used different signal intensity based thresholds in different aneurysms, without explicitly investigating the robustness of the aneurysm segmentation for various thresholds. Rather, we focused on the effect of signal intensity fluctuations to give a more in-depth analysis of the behavior of the pulsation estimation as function of the image characteristics. The segmentation depends on the actual CNR in combination with the signal intensity fluctuations. The threshold should be high enough to avoid including noise, but not too high to prevent exclusion of aneurysm pixels. Ignoring partial volume effects and assuming normal distributed noise, it is fairly straightforward to analyze the sensitivity of the segmentation to the chosen threshold. If less than 1% of the included pixels in the segmentation is allowed to be due to noise, the lower limit of the intensity threshold is approximately 2.5 x SD (where SD = the standard deviation of the noise). Increasing the threshold further would change the volume by less than 1%, provided that the threshold is not exceeding the upper limit where the aneurysm intensity will start failing to pass the threshold. Similarly, the upper limit would be ((1-f)*CNR-2.5)*SD), where f is the intensity fluctuation as fraction of the aneurysm signal (note that CNR*SD is the intensity of the aneurysm). From this simple reasoning, it would follow that a minimum CNR of 5 is

required to allow robust segmentation without suffering too much from noise, which matches with the phantom simulations, which showed that the accuracy dropped quickly below a CNR of 6. Nonetheless, voxels with partial volume effect should be considered as well. They have an intensity somewhere in between the aneurysm intensity and the noise level, depending on the partial volume factor. Basically, the threshold determines how 'full' a voxel should be to be counted as aneurysm voxel. In these voxels, intensity fluctuation is directly related to how many partial volume voxels will pass the intensity threshold. Thus, changing the threshold will lead to a change in (baseline) volume. However, as each partial volume fraction is equally likely to occur, the sensitivity to intensity fluctuations and to actual volume changes is not expected to depend on the chosen threshold.

This study has some limitations. First, we used a signal intensity based threshold to segment the aneurysm volume, but also showed that signal intensity fluctuations have a considerable influence on the accuracy of the volume pulsation analysis. Future studies should use an analysis method which is insensitive to signal intensity fluctuations throughout the cardiac cycle. For example, a recently published automatic segmentation method used for quantification and visualization of pulsation from electrocardiography-gated CTA data, uses the local deformation of image structures in all cardiac phases, which may be less dependent on the actual intensity.10 By using such an automated method, the effects of manual correction are also eliminated, and the precision of the measurement may be increased. Second, our estimate of aneurysm-specific inaccuracy was based on patient-specific measurements of CNRs and intensity fluctuations. Although care was taken to obtain representative values, one should note that both the CNR and intensity fluctuations may be variable along the border of the aneurysm. Also, the CNR measurements were likely influenced by intensity fluctuations. Since there was no separate noise acquisition in the MRI protocol, we used the SD of the region of interest over the cardiac cycles, which may have led to an underestimation of the actual CNR (and, thus, to a slightly worse inaccuracy than actually present). Nonetheless, the accuracy analysis shows that aneurysm-specific inaccuracies should be determined, and that an increase in the signal-to-noise ratio of the images should be achieved to improve the accuracy. Third, our restricted FOV led to incomplete imaging of the largest aneurysm of 19 mm in stage I of the study, and the subsequent pulsation only accounts for the imaged part. We were not able to expand the FOV due to a fixed scan protocol and therefore fixed scantime. In the second stage of this study, we were able to increase the FOV to prevent this lack of coverage. Fourth, we found quite large differences in volume pulsation in stage II of the study compared to stage I. We cannot exclude that this is a reflection of an actual difference between aneurysms as a different sample of patients was used in stage II, which is not optimal when investigating an optimized imaging sequence. However, the most likely explanation is the substantial increase in signal intensity fluctuations in stage II compared to stage I, despite the aim to increase CNR and decrease intensity fluctuations. Higher signal intensity pulsation leads to a decrease in volume pulsation quantification accuracy and this is probably an important reason why a higher pulsation was measured in the aneurysms with the improved TFE in stage II. Furthermore, the lower volume pulsation found in the same aneurysms on the contrast enhanced TFE compared to the improved TFE can also be explained by lower signal intensity fluctuations in the contrast enhanced TFE. Since lower signal intensity leads

to increased accuracy of the volume pulsation quantification, the results of the contrast enhanced TFE were considered more accurate than the results of the improved TFE. Nonetheless, the intensity pulsations with the contrast enhanced TFE are still considerable (ranging from 7.5 to 24%), which is still too high to make volume pulsation analysis on this sequence accurate. Last, the clinical availability of 7T MRI is still limited but expected to increase in the future.

The strength of this study is the use of an advanced high resolution imaging method to quantify pulsation in aneurysms, combined with a thorough accuracy analysis. All previous studies showed a single value for the inaccuracy, sometimes obtained from a large stable phantom. The phantom simulations in our study give insight in the relative contributions of different sources of measurement errors, and their combined effect in a patient-specific way, which can stimulate future improvement on each of these aspects. An advantage of MR over CTA is the lack of radiation for MRI. Furthermore, the ultra-high resolution of MRI combined with its ability to discriminate the aneurysm wall from its lumen, provides a unique opportunity to search for new markers of rupture.

Conclusions

In conclusion, quantification of intracranial aneurysm pulsation seemed to be feasible with 7T MRI, but even after optimization of the imaging protocol the artifactual volume pulsations as a result of intensity fluctuations, the limited CNR, aneurysm size, and the flow displacement artifact have the same magnitude as the volume pulsations observed in the patient data. The current imaging protocol on 7T MRI is therefore of no use in studying pulsation as a risk factor for rupture at the moment. Future studies should always include an aneurysm-specific accuracy analysis.

Supplementary Material

Refer to Web version on PubMed Central for supplementary material.

Acknowledgements

We acknowledge A. Zada and B. de Vries for their work on the accuracy analysis.

Grant support: R. Kleinloog was supported by a ‘Focus en Massa’ cardiovascular research grant by the University Utrecht, the Netherlands. Y.M. Ruigrok was supported by a clinical fellowship grant by the Netherlands Organization for Scientific Research (NWO) (project no. 40-00703-98-13533). J.J.M. Zwanenburg was supported by the European Research Council under the European Union's Seventh Framework Programme (FP7/2007-2013) / ERC grant agreement n°337333.

This manuscript has not been submitted elsewhere nor published elsewhere in whole or in part, except as an abstract (poster on European Stroke Conference 2013, on Vasospasm 2013 and on International Society for Magnetic Resonance in Medicine (ISMRM) 2014).

Abbreviation Key

TFE	Turbo Field Echo
CNR	contrast-to-noise-ratio

PCMR	phase-contrast MR imaging
SD	standard deviation

References

1. Vlak MH, Algra A, Brandenburg R, et al. Prevalence of unruptured intracranial aneurysms, with emphasis on sex, age, comorbidity, country, and time period: a systematic review and meta-analysis. Lancet Neurol. 2011; 10:626–636. [PubMed: 21641282]
2. Nieuwkamp DJ, Setz LE, Algra A, et al. Changes in case fatality of aneurysmal subarachnoid haemorrhage over time, according to age, sex, and region: a meta-analysis. Lancet Neurol. 2009; 8:635–642. [PubMed: 19501022]
3. Brinjikji W, Rabinstein AA, Nasr DM, et al. Better outcomes with treatment by coiling relative to clipping of unruptured intracranial aneurysms in the United States, 2001-2008. AJNR Am J Neuroradiol. 2011; 32:1071–1075. [PubMed: 21511860]
4. Naggara ON, Lecler A, Oppenheim C, et al. Endovascular treatment of intracranial unruptured aneurysms: a systematic review of the literature on safety with emphasis on subgroup analyses. Radiology. 2012; 263:828–835. [PubMed: 22623696]
5. Vanrossomme AE, Eker OF, Thiran JP, et al. Intracranial Aneurysms: Wall Motion Analysis for Prediction of Rupture. AJNR Am J Neuroradiol. 2015; 36:1796–1802. [PubMed: 25929878]
6. Kleinloog R, Korkmaz E, Zwanenburg JJ, et al. Visualization of the aneurysm wall: a 7.0-tesla magnetic resonance imaging study. Neurosurgery. 2014; 75:614–622. [PubMed: 25255252]
7. van Ooij P, Zwanenburg JJ, Visser F, et al. Quantification and visualization of flow in the Circle of Willis: time-resolved three-dimensional phase contrast MRI at 7 T compared with 3 T. Magn Reson Med. 2013; 69:868–876. [PubMed: 22618854]
8. Bland JM, Altman DG. Applying the right statistics: analyses of measurement studies. Ultrasound Obstet Gynecol. 2003; 22:85–93. [PubMed: 12858311]
9. Larson TC 3rd, Kelly WM, Ehman RL, et al. Spatial misregistration of vascular flow during MR imaging of the CNS: cause and clinical significance. AJNR Am J Neuroradiol. 1990; 11:1041–1048. [PubMed: 2120979]
10. Firouzian A, Manniesing R, Metz CT, et al. Quantification of Intracranial Aneurysm Morphodynamics from ECG-gated CT Angiography. Acad Radiol. 2013; 20:52–58. [PubMed: 22884403]
11. Kuroda J, Kinoshita M, Tanaka H, et al. Cardiac cycle-related volume change in unruptured cerebral aneurysms: a detailed volume quantification study using 4-dimensional CT angiography. Stroke. 2012; 43:61–66. [PubMed: 21998064]
12. Illies T, Saering D, Kinoshita M, et al. Feasibility of quantification of intracranial aneurysm pulsation with 4D CTA with manual and computer-aided post-processing. PLoS One. 2016; 11:e0166810. [PubMed: 27880805]

Europe PMC Funders Author Manuscripts

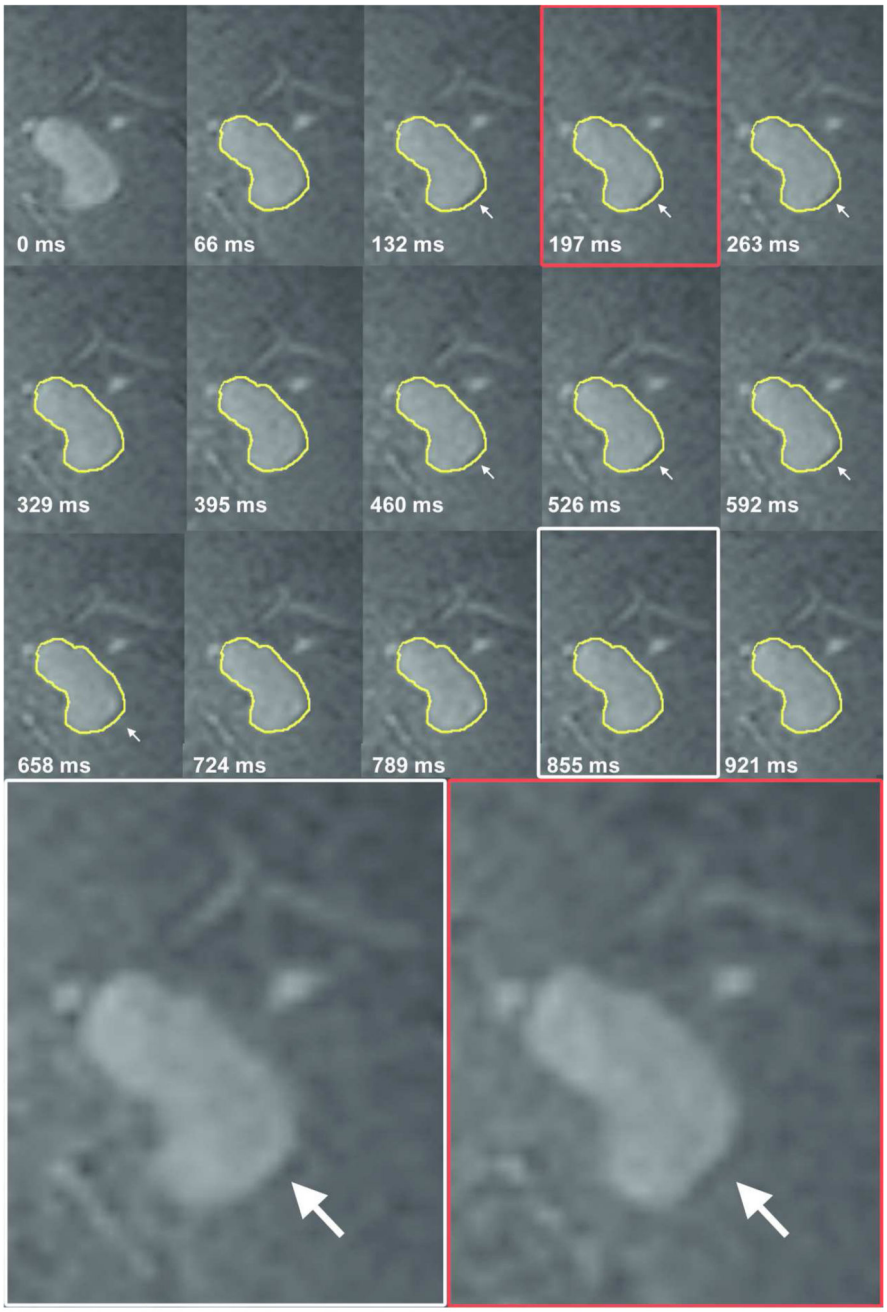

Figure 1.

Coronal cross-section of a left middle cerebral artery aneurysm for each of the 15 phases of the cardiac cycle (heart rate 60 beats per minute). The contour of the aneurysm at 0 ms is shown in yellow on all other time points. The white arrows indicate the area of pulsation in this cross-section. Magnification of two phases shows the deformation of the aneurysm at one side of the dome.

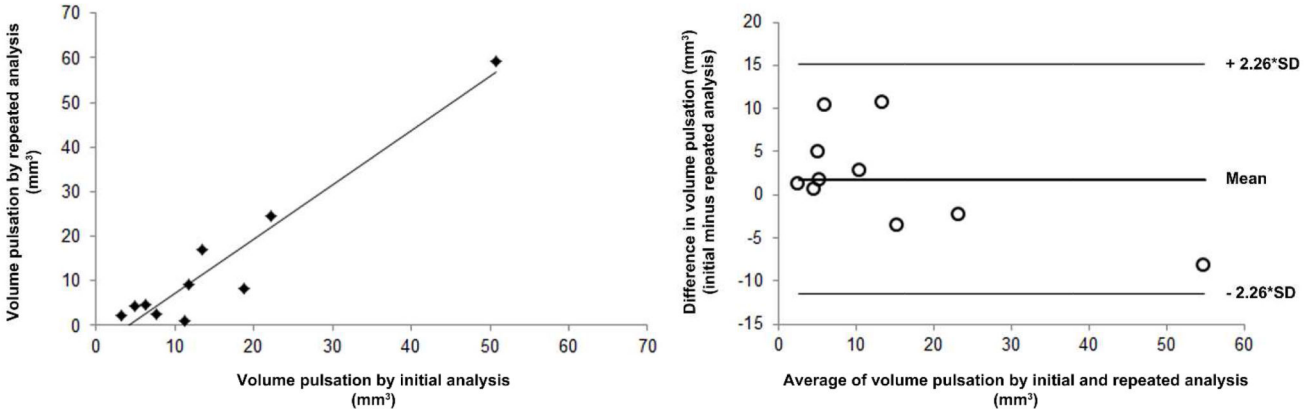

Figure 2.

Repeatability of the image analysis method.

Left: scatterplot showing the correlation between the measured volume pulsation obtained with the repeated image analysis vs. the results from the initial analysis. Right: Bland-Altman plot of the same data. SD indicates standard deviation.

Europe PMC Funders Author Manuscripts

Europe PMC Funders Author Manuscripts

Table 1

Overview of the three different sequences used to image volume pulsation and the main results.

	Stage I	Stage II	
Sequence	TFE	Improved TFE	CE - improved TFE
Number of phases in the cardiac cycle	15	18	18
Number of patients included	9	9	8*
Number of aneurysms included	10	9	8*
Mean size of the aneurysms in mm (SD, range)	9 (4, 3-19)	8 (4, 2-14)	8 (4, 2-14)
Mean aneurysm volume change in mm^3 (SD, range)	15 (14, 3-51)	38 (31, 2-88)	14 (9,1-25)
Mean volume pulsation in % (SD, range)	8 (7, 2-27)	39 (24, 14-73)	15 (11, 4-36)
Mean absolute observed artifactual pulsation in mm^3 (SD, range)	2 (2, 0-5)	-	13 (9, 1-27)

CE indicates contrast enhanced.

*In one patient, the image acquisition of the contrast enhanced improved TFE failed.

Europe PMC Funders Author Manuscripts

Table 2

Baseline characteristics and pulsation of the ten unruptured intracranial aneurysms in stage I.

Aneurysm number	Aneurysm size in mm, largest diameter (height x width)	Age, sex	Location aneurysm	Imaging sequence	Minimum volume (mm^3)	Moment of minimum volume in the cardiac cycle (% of cardiac cycle)	Maximum volume (mm^3)	Moment of maximum volume in the cardiac cycle (% of cardiac cycle)	Relative volume pulsation (%)	Absolute volume pulsation (mm^3)	Absolute observed artifactual pulsation (mm^3) #
1	2.8 (1.8x1.6)	56, F	Pericallosal	TFE	12	93	15	20	25	3	1.3
2	5.6 (4.5x3.9)	60, F *	Pericallosal	TFE	70	93	75	53	7	5	1.9
3	6.1 (6.1x5.7)	74, F	ACOM	TFE	92	100	98	53	7	6	3.1
4	6.8 (6.0x4.7)	60, F *	MCA	TFE	56	40	64	13	14	8	0.7
5	8.7 (6.1x7.7)	72, F	PICA	TFE	308	7	327	73	6	19	-0.2
6	9.3 (6.6x8.2)	56, F	ACOM	TFE	292	100	303	20	4	11	1.1
7	9.6 (6.1x9.6)	55, M	MCA	TFE	285	40	298	73	5	13	5.4
8	10.1 (8.8x7.7)	64, M	MCA	TFE	276	53	298	13	8	22	-0.4
9	12.9 (12.9x6.3)	50, F	MCA	TFE	312	13	324	27	4	12	2.6
10	18.6 (14x15.8)	53, F	Basilar	TFE	2078	47	2128	100	2	50	3.5

* Two aneurysms in one patient. MCA indicates middle cerebral artery; ACOM, anterior communicating artery; PICA, posterior inferior cerebellar artery.

The absolute observed artifactual pulsation is the difference between the absolute volume pulsation and the volume pulsation of the aneurysm-specific digital phantom, and is a measure for the inaccuracy of the volume pulsation analysis (see supplementary material for further details).

Europe PMC Funders Author Manuscripts

Table 3

Baseline characteristics and pulsation of the nine unruptured intracranial aneurysms in stage II.

Aneurysm number	Aneurysm size in mm, largest diameter (height x width)	Age, sex	Location aneurysm	Imaging sequence	Minimum volume (mm^3)	Moment of minimum volume in the cardiac cycle (% of cardiac cycle)	Maximum volume (mm^3)	Moment of maximum volume in the cardiac cycle (% of cardiac cycle)	Relative volume pulsation (%)	Absolute volume pulsation (mm^3)	Absolute observed artifactual pulsation (mm^3) *
11	2 (2x1.6)	53, F	MCA	TFEi	3	22	4	6	73%	2	-
				CE TFEi	2	22	3	94	36%	1	2
12	6.2 (5.1x3.3)	58, F	MCA	TFEi	68	28	90	6	31%	21	-
				CE TFEi	96	33	104	6	8%	8	1
13	5.4 (4.8x4.4)	70, M	ACOM	TFEi	44	78	75	100	70%	31	-
				CE TFEi	78	78	96	100	23%	18	13
14	5.7 (5.7x3.1)	47, F	MCA	TFEi	62	28	79	94	28%	17	-
				CE TFEi	70	22	78	89	11%	8	9
15	8.7 (8.1x6)	39, M	MCA	TFEi	134	83	153	17	14%	19	-
				CE TFEi	NA	NA	NA	NA	NA	NA	NA
16	8.7 (7.9x5.4)	70, M	ACOM	TFEi	91	72	149	94	64%	58	-
				CE TFEi	114	72	138	100	22%	25	27
17	9.4 (8.7x6.7)	53, M	ACOM	TFEi	188	89	215	11	14%	27	-
				CE TFEi	256	83	265	100	4%	9	10
18	12.3 (8.1x8)	70, M	ACOM	TFEi	206	78	289	94	41%	84	-
				CE TFEi	166	78	191	94	15%	25	24
19	13.7 (10.9x8.7)	51, M	ACOM	TFEi	419	22	507	89	21%	88	-
				CE TFEi	581	22	603	94	4%	22	25

MCA indicates middle cerebral artery; ACOM, anterior communicating artery; TFEi, the improved version of the Turbo Field Echo sequence to image pulsation used in stage II; CE, contrast enhanced.

* The absolute observed artifactual pulsation is the difference between the absolute volume pulsation and the volume pulsation of the aneurysm-specific digital phantom, and is a measure for the inaccuracy of the volume pulsation analysis (see supplementary material for further details). Only the contrast enhanced TFE data was used as input for the phantom experiment, because we expected the contrast enhanced TFE sequence to perform better than the improved TFE alone.